Electronic Supplementary Material (ESI) for Soft Matter.

Supporting Information

Modulating interfacial attractions of polymer-grafted nanoparticles in melts under shear

Erkan Senses, Yang Jiao and Pinar Akcora*

Department of Chemical Engineering & Materials Science, Stevens Institute of Technology

Hoboken NJ 07030 USA

Corresponding author: pakcora@stevens.edu

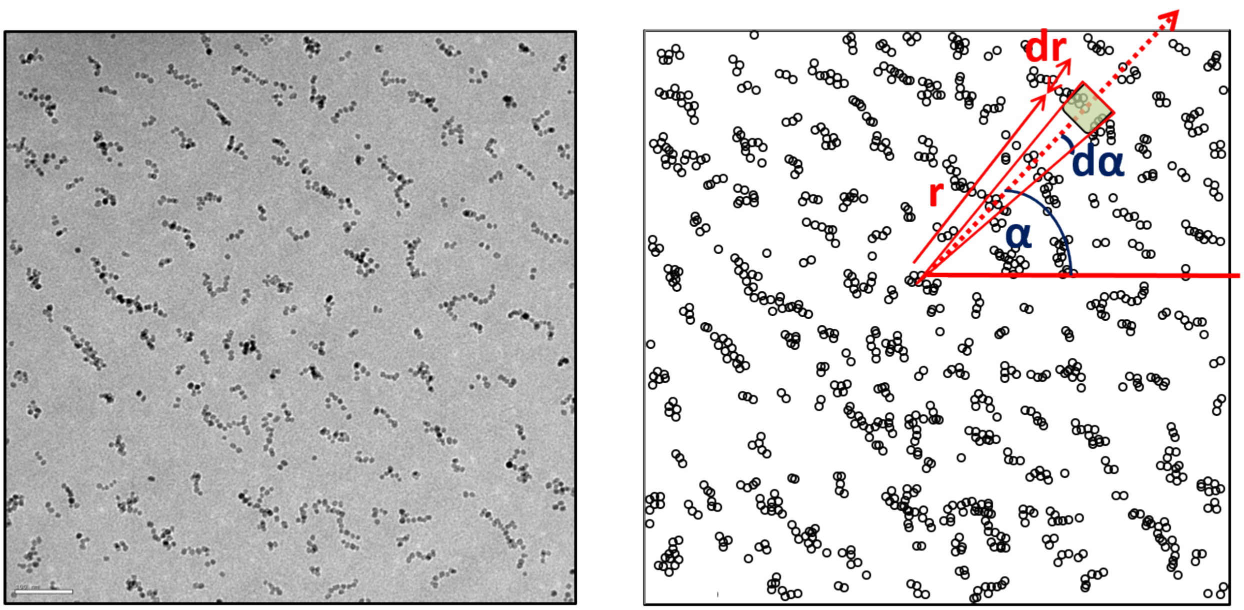

Figure S1. TEM micrograph of PS-grafted iron oxide NPs dispersed in PS matrix and representation of the located particles used in the calculation of particle pair distribution functions. The angular and radial variations are displayed with respect to a particle.

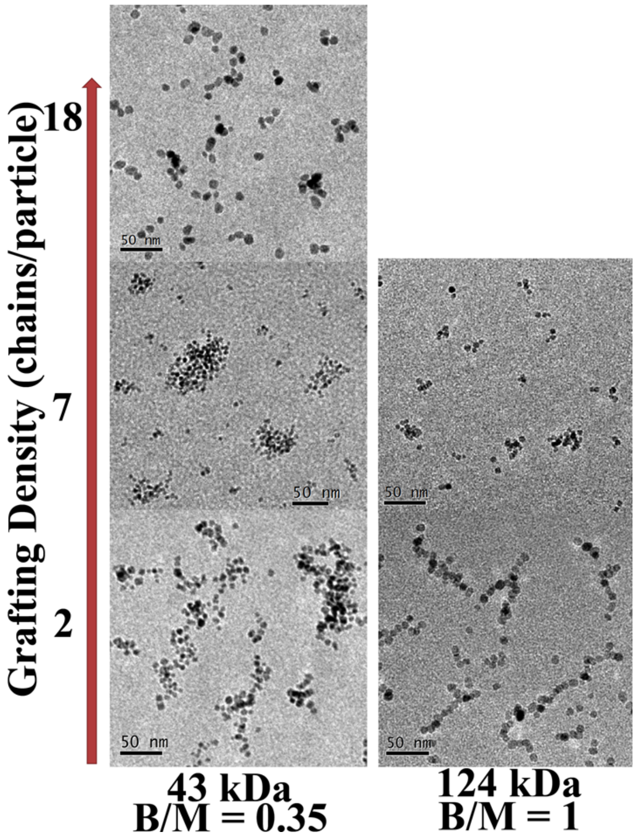

Figure S2. TEM images show transition of nanostructures from large elongated branched chains to spheres and to short chains with the increase of grafting density from bottom to top[1]. The first column is for 43 kg/mol PS-grafted nanoparticles with 0.017 (bottom), 0.044 (middle) and 0.066 chains/nm^2 (top) grafting densities. The second column is for 124 kg/mol graft with 0.052 chains/nm^2 (top) and 0.013 chains/nm^2 (bottom) densities. Particles are dispersed in 124 kg/mol PS matrix in all samples.

Nonlinear Results on Homopolymer: Total stress-strain (Lissajous) plots of PS homopolymer (124 kg/mol) deformed at different strain amplitudes at 1 rad/s frequency are presented in Figures S2a-b. Total stress includes higher order harmonic contributions; thus, elastic and viscous stresses cannot be directly obtained by calculating the in-phase and out-of phase components. The elliptic shape of stress is distorted indicating the presence of nonlinearities in stress response. Total stress response can be represented in Fourier series that combine elastic and viscous stress components[2,3,4]. We have decomposed the total stress into its odd (σ’) and even (σ”) parts to represent the elastic and viscous behavior of a material in nonlinear regime[5]:

$$\sigma'(t) = \left[\sigma(t) - \sigma(-t)\right]/2 \qquad\qquad \sigma''(t) = \left[\sigma(t) + \sigma(-t)\right]/2$$

The resulting stress functions are no longer loops but reduced to a single-valued function as shown in Figure 4b with time. These viscous and elastic stresses are conveniently represented in a Fourier space, $\sigma(t,\omega;\gamma_0) = \gamma_0 \sum_{n=odd} \left[G_n^{'}\sin(n\omega t) + G_n^{''}\cos(n\omega t)\right]$, where $G_1^{'}$ and $G_1^{''}$ are the average storage and loss moduli for a given cycle. Local moduli at small (G_S) and large (G_L) strain within a cycle of deformation can be obtained from the slopes of the curves as[2];

$$G_L = \lim_{\gamma \to \gamma_0}(\sigma'(\gamma)/\gamma) \qquad G_S = \lim_{\gamma \to 0}(\sigma'(\gamma)/\gamma)$$

The positive deviations at large strains represent strain-stiffening ($G_L > G_S$) which is shown in Figure S2c. The strain amplitude 100% is chosen for nonlinear tests in order to underpin the effect of entanglements on stiffening because average elastic modulus ($G_1^{'}$) and local moduli decay beyond 200% strain amplitudes due to effective disentanglement of polymer chains as presented in Figure S3d.

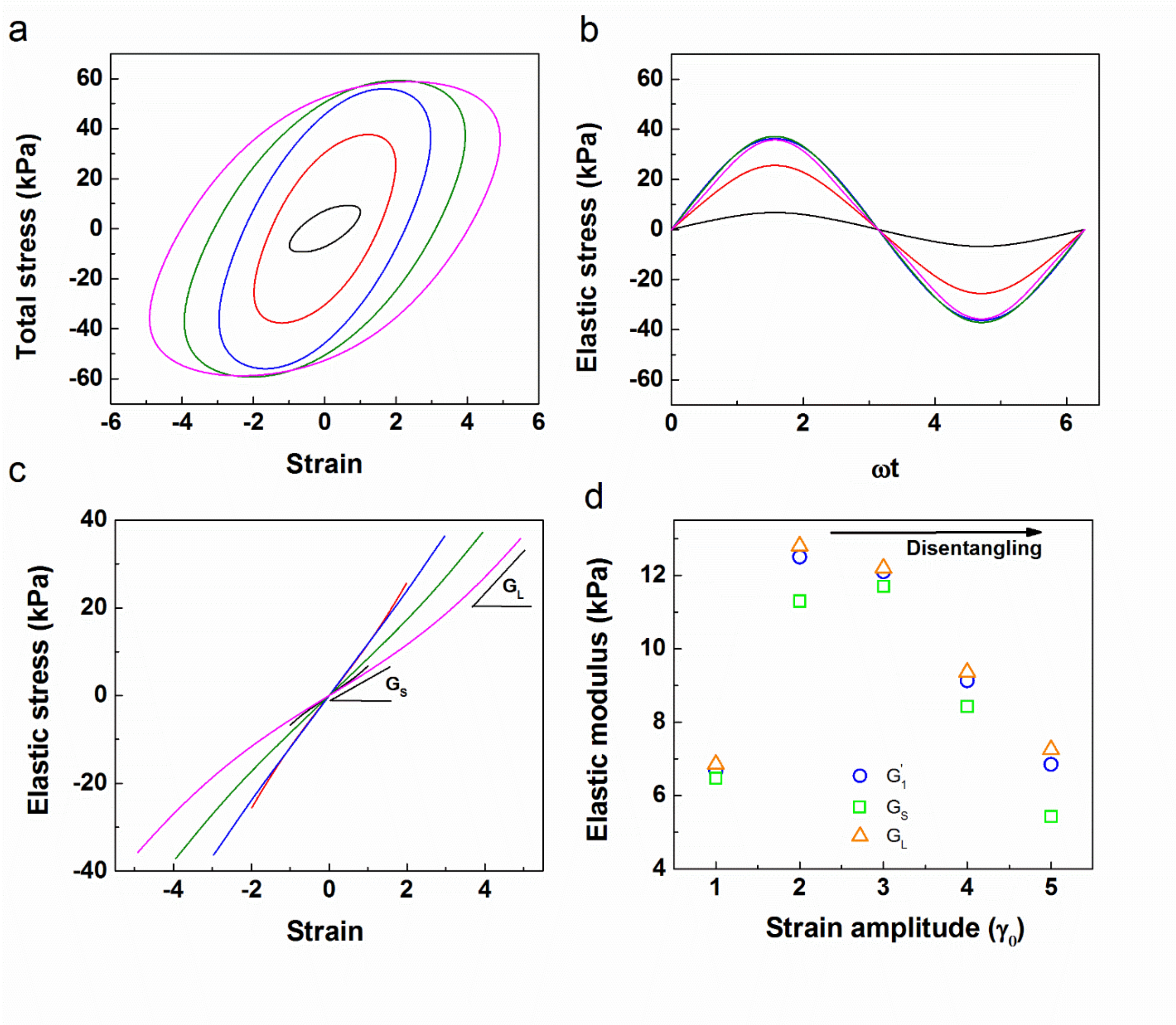

Figure S3. (a) Elastic Lissajous curves obtained for 124 kg/mol PS homopolymer at varying strain amplitudes (100%-500%, represented in different colors). The elliptic shape of the curves is distorted with nonlinearities in the stress response at large strain values. **(b)** Decomposed elastic stress response within a cycle of deformation displays periodic non-linear behavior. **(c)** Elastic stress response to instantaneous strain within a cycle of deformation shows strain-stiffening at large strains, resulting in different modulus at small (G_S) and large (G_L) strains. **(d)** Comparison of the first harmonic average modulus in nonlinear regime ($G_1^{'}$) and the local moduli (G_S and G_L) as a function of strain.

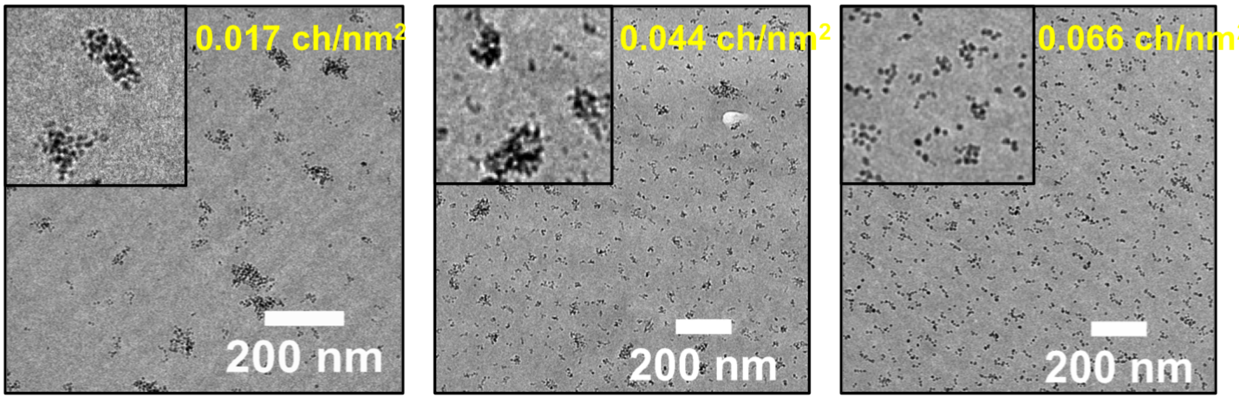

Figure S4. TEM micrographs of composite with 43 kg/mol PS-grafted NPs of various grafting densities in 124 kg/mol matrix after shearing at 100% strain at 1 rad/s.

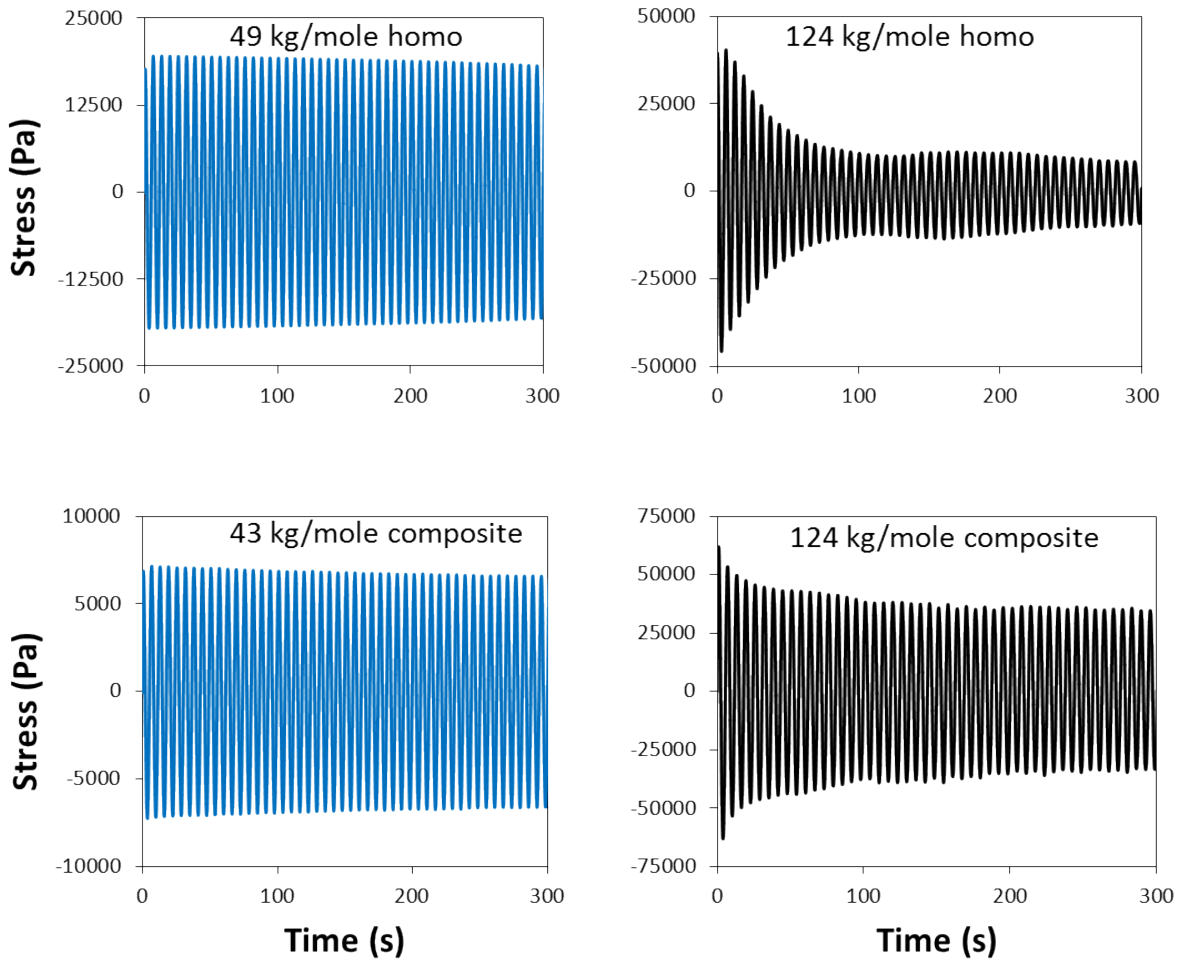

Figure S5. Raw stress-time data for homopolymers with 49 kg/mol and 124 kg/mol and their composites prepared with 43 kg/mol (graft density 0.017 chains/nm^2) and 124 kg/mol (graft density 0.013 chains/nm^2) PS-grafted NPs.

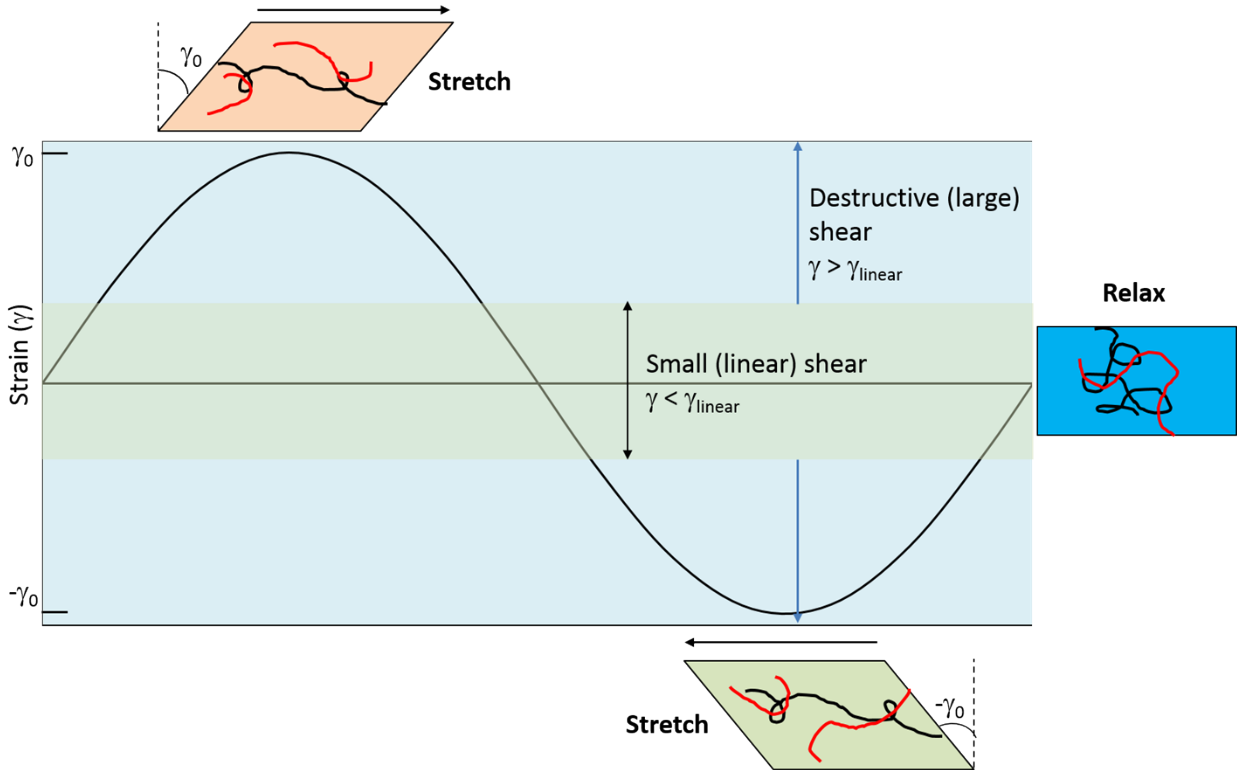

Figure S6. Schematic drawing of cyclic chain deformations under large amplitude oscillatory shear (LAOS). Unlike steady shear experiments where strain increases in time with a constant rate, in LAOS polymer chains repeatedly stretch and relax as strain oscillates between linear and nonlinear regions as shown. This cyclic chain stretching-relaxation process facilitates the entanglement of long matrix chains with the short grafted chains.

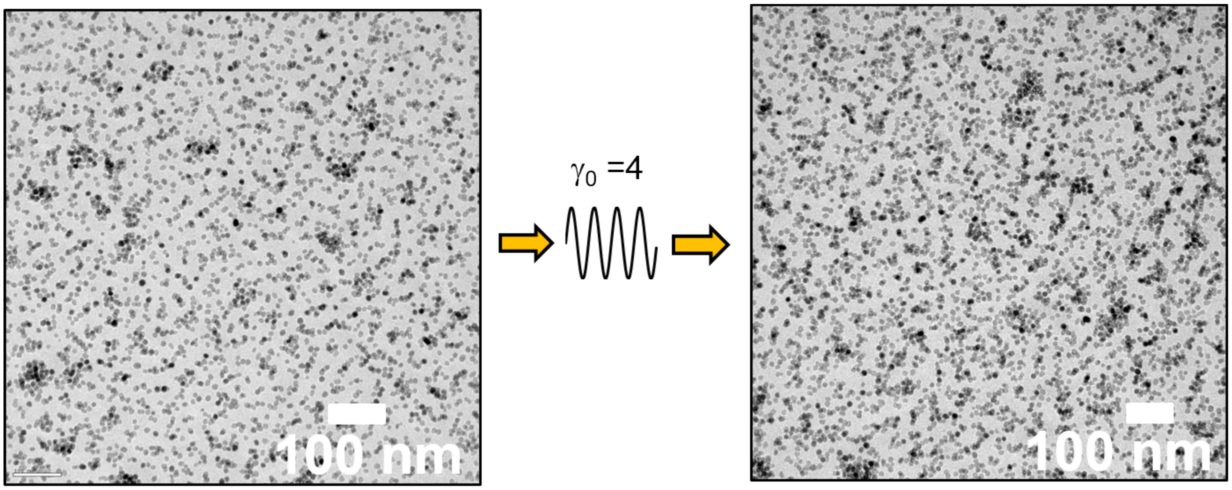

Figure S7. Dispersions in as-cast and deformed composite with 15 wt% filler loading. Deformation is applied at 400% strain in 119 kg/mol PS grafted NP in 130 kg/mol PS matrix.

Table S1. Sample characteristics of PS homopolymers and grafted particles used in this work. Viscoelastic data of composites prepared from polymer-grafted iron oxide NPs (5 wt% loading) at 100% strain amplitude and 150°C. (*) labeled samples contain 15 wt% loading.

Grafted Chain M.W. (kg/mol)	*Graft density (chains/nm^2)*	*Matrix M.W. (kg/mol)*	*G_1' (Pa)*	*G_1" (Pa)*
124 (PDI: 1.28)	*0.013*	*124*	*24300*	*26100*
124	*0.013*	*43*	*1960*	*12900*
124	*0.013*	*15 (PDI: 1.06)*	*92.2*	*543*
124	*0.05*	*124*	*38000*	*37200*
**119 (PDI: 1.07)*	*0.016*	*130 (PDI: 1.08)*	*32339*	*33536*
**95 (PDI: 1.07)*	*0.074*	*130*	*29642*	*23247*
**45 (PDI: 1.11)*	*0.12*	*130*	*31672*	*27557*
43 (PDI: 1.06)	*0.017*	*124*	*6950*	*11600*
43	*0.044*	*124*	*29700*	*28800*
43	*0.066*	*124*	*35900*	*31300*
43	*0.017*	*43*	*524*	*6568*
43	*0.044*	*43*	*1180*	*10264*
43	*0.066*	*43*	*728*	*6200*
		124 (homo) (PDI: 1.28) *15 (homo)* *49k (homo) (PDI: 1.1)*	*6670* *269* *2940*	*7090* *1798* *18250*

REFERENCES

(1) Jiao, Y.; Akcora, P. *Macromolecules* **2012**, *45*, 3463.
(2) Ewoldt, R. H.; Hosoi, A. E.; McKinley, G. H. *Journal of Rheology* **2008**, *52*, 1427.
(3) Wilhelm, M. *Macromolecular Materials and Engineering* **2002**, *287*, 83.
(4) Neidhöfer, T.; Wilhelm, M.; Spiess, H. W. *Applied Rheology* **2001**, *11*, 126.
(5) Cho, K. S.; Hyun, K.; Ahn, K. H.; Lee, S. J. *Journal of Rheology* **2005**, *49*, 747.